Current Biology, *Volume 22*

Supplemental Information

Phosphatidylinositol-3-Phosphate Clearance Plays a Key Role in Autophagosome Completion

Eduardo Cebollero, Aniek van der Vaart, Mantong Zhao, Ester Rieter, Daniel J. Klionsky, J. Bernd Helms, and Fulvio Reggiori

Supplemental Experimental Procedures

Strains and media

The *S. cerevisiae* strains used in this study are listed in Table S1. For gene disruptions, the entire *ATG1*, *ATG4, ATG9, ATG13, ATG14, PEP4* and *VAM3* coding regions were replaced with the *HIS3*, *TRP1*, *LEU2* or *URA3* genes amplified from the series of pUG template plasmids using PCR primers containing ~60 bases of identity to the regions flanking the open reading frames to be deleted [1]. Gene knockouts were verified by PCR or western blot using specific antibodies. Antiserum against Atg1 has been described elsewhere [2]. Pep4 antibody was generated by immunization of New Zealand White rabbits with the CDLTIPKQDFAEAT peptide (New England Peptide, Gardner, MA). Integrations of the gene encoding GFP at the 3' end of *YMR1*, *SJL3*, *ATG2*, *ATG9*, *ATG14*, *ATG16*, *ATG17*, *ATG18*, *OM45* and *PEX14* were performed as described previously [3].

Yeast cells were grown in rich (YPD; 1% yeast extract, 2% peptone, 2% glucose) or synthetic minimal (SMD; 0.67% yeast nitrogen base, 2% glucose, amino acids and vitamins as needed) media. Starvation experiments were conducted in synthetic medium lacking nitrogen (SD-N; 0.17% yeast nitrogen base without amino acids, 2% glucose) or by addition of 0.2 μg/ml rapamycin (LC Laboratories, Woburn, MA) to the culture.

Plasmids

The *YMR1* gene, including the endogenous promotor and terminator sequences, was cloned as a *Kpn*I/*Sac*I fragment into the pRS416 centromeric vector to generate the pYMR1(416) plasmid [4]. Similarly, the pSJL3(426) plasmid expressing Sjl3 was cloned as a *Xho*I/*Sac*II fragment into the pRS426 multicopy vector [4]. The pYMR1MUT(416) plasmid expresses a phosphatase-dead allele of *YMR1* that contains a point mutation changing the cysteine 397 of Ymr1 into a serine, which was introduced by quick-change mutagenesis into the pYMR1(416) plasmid [5].

The integrative pYMR1GFP406 plasmid was generated by sequentially cloning into the pRS406 plasmid the *YMR1* promoter, the *YMR1* ORF and *GFP* as *Xho*I-*SnaB*I, *SnaB*I-*Aat*II, *Aat*II-*Sac*I fragments, respectively. This plasmid was used as a template to create the pYMR1C397SGFP406 vector expressing Ymr1^{C397S}-GFP by quick-change mutagenesis, and the pNΔYMR1GFP406 vector carrying a truncated version of Ymr1-GFP generated by replacing *YMR1* with a PCR-generated *SnaB*I-*Aat*II *YMR1* fragment lacking the 147 amino acids N-terminal sequence coding for the PH-GRAM domain.

The pCuGFPATG8416 and pCuGFPATG8415 plasmids have been described elsewhere [6], as well as the pPS130 plasmid allowing the integration of the *RFP-APE1* construct [7] and the pCuV5mCherryAtg8415 plasmid [8].

Fluorescence microscopy

Autophagy was induced by addition of rapamycin for 3 h to cells grown in SMD medium before visualizing fluorescence signals with a DeltaVision RT fluorescence microscope (Applied Precision, Issaquah, WA) equipped with a CoolSNAP HQ camera (Photometrix, Tucson, AZ). Images were generated by collecting a stack of 20 pictures with focal planes 0.20 µm apart in order to cover the entire volume of a yeast cell and by successively deconvolving them using SoftWoRx software (Applied Precision). A single focal plane is shown at each time point. The number of mChe-Atg8-positive puncta per cell was counted in 50 cells from 2 independent experiments. To establish the degree of colocalization between Atg8 and the various analyzed Atg proteins, the number of mChe-Atg8 puncta positive for the GFP signal was also counted in 50 cells from 2 independent experiments. In the same cells, the number of GFP-tagged Atg protein puncta was also determined. A single focal plane is shown at each time.

Measurement of the GFP-Atg8 cycle duration and the signal intensity at the PAS was carried out as previously described [9]. In brief, to determine signal intensity, the time point at which the punctate structure could first be seen was set as time 1 and fluorescence intensity at this time point was normalized to 1. To measure the intensity, a small circle was drawn around the dot and another circle with the same size was drawn at an adjacent cytosolic area to be used as background and subtracted.

Electron microscopy

Cells were processed for EM as described previously [10]. To determine the number of autophagic bodies per vacuole and autophagosomes per cell profile, two different grids with sections obtained from the same preparation were evaluated. For every grid, the number of either autophagic bodies or autophagosomes in 60 cells with apparent vacuoles was counted. Error bars represent the standard deviation from the counting of the two grids.

Miscellaneous procedures

The protease protection assay, GFP-Atg8 processing, Pho8Δ60 activity measurement, pexophagy and mitophagy assays, and protein extraction and western blot analyses were conducted as previously described [11-15]. Western blot results were quantified using an Odyssey infrared imaging system (Li-Cor Biosciences, Lincoln, NE).

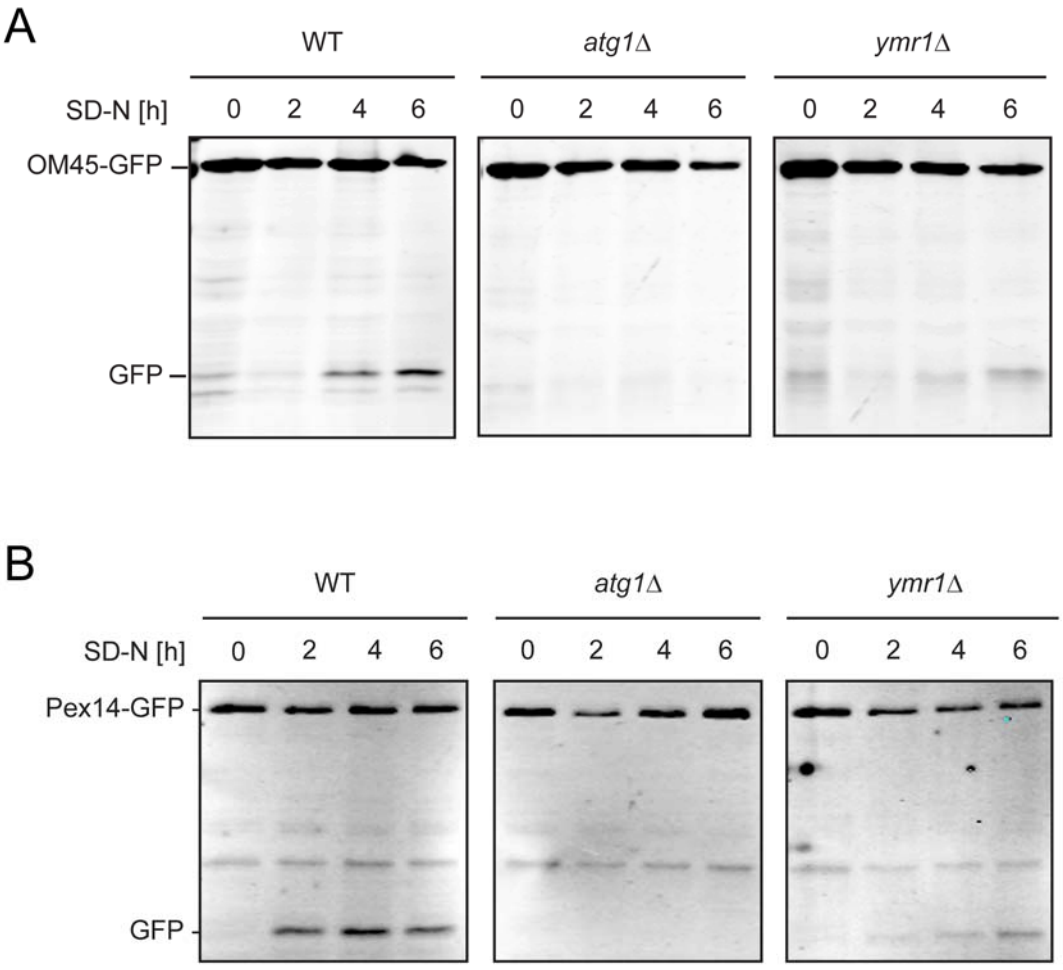

Figure S1. Ymr1 is required during selective-types of autophagy. (A) Mitophagy assay. WT (ECY129), *atg1*Δ (ECY133) and *ymr1*Δ (ECY127) strains that express endogenous Om45-GFP were incubated in a lactate-containing medium to induce the proliferation of mitochondria before triggering mitophagy by transferring the cells to SD-N medium for 6 h. Om45-GFP cleavage was determined every 2 h by western blot using anti-GFP antibodies. (B) Pexophagy assay. WT (ECY131), *atg1*Δ (ECY103) and *ymr1*Δ (ECY134) strains expressing endogenous Pex14-GFP were grown in an oleate-containing medium to stimulate the production of peroxisomes before inducing pexophagy and measuring Pex14-GFP processing similar to the method used in panel (A).

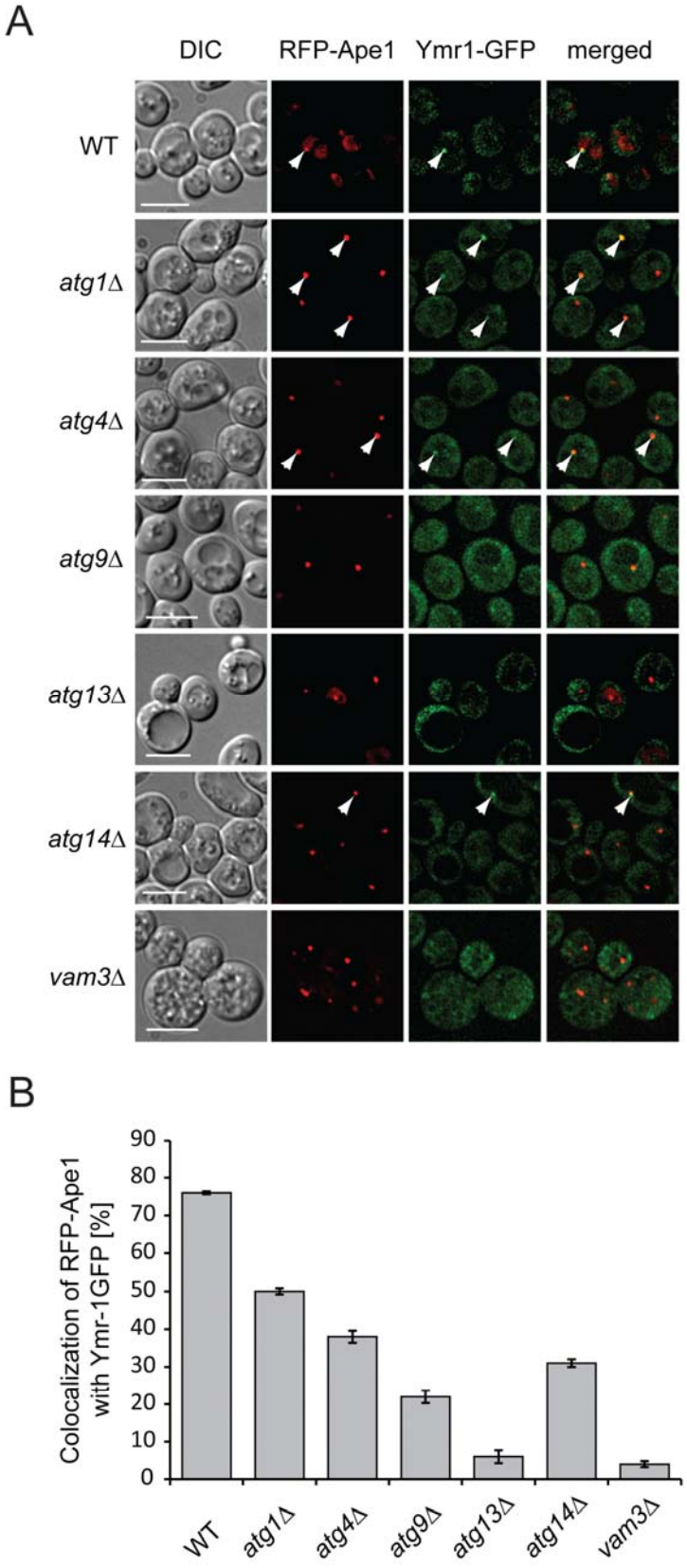

Figure S2. Ymr1 is recruited at the early stages of PAS formation. (A) WT (ECY202), *atg1*Δ (ECY208), *atg4*Δ (ECY209), atg9Δ (ECY221), *atg13*Δ (ECY222), *atg14*Δ (ECY211) and *vam3*Δ (ECY212) cells expressing RFP-Ape1 and Ymr1-GFP were grown to an early log phase before transferring them into SD-N medium for 3 h to induce autophagy followed by image collection. Arrowheads highlight colocalization. DIC, differential interference contrast. Scale bar, 5 μm. (B) Quantification of the degree of colocalization between the GFP-tagged proteins and RFP-Ape1 in the samples imaged in panel B. The graphs represent the average of 2 experiments ± SEM.

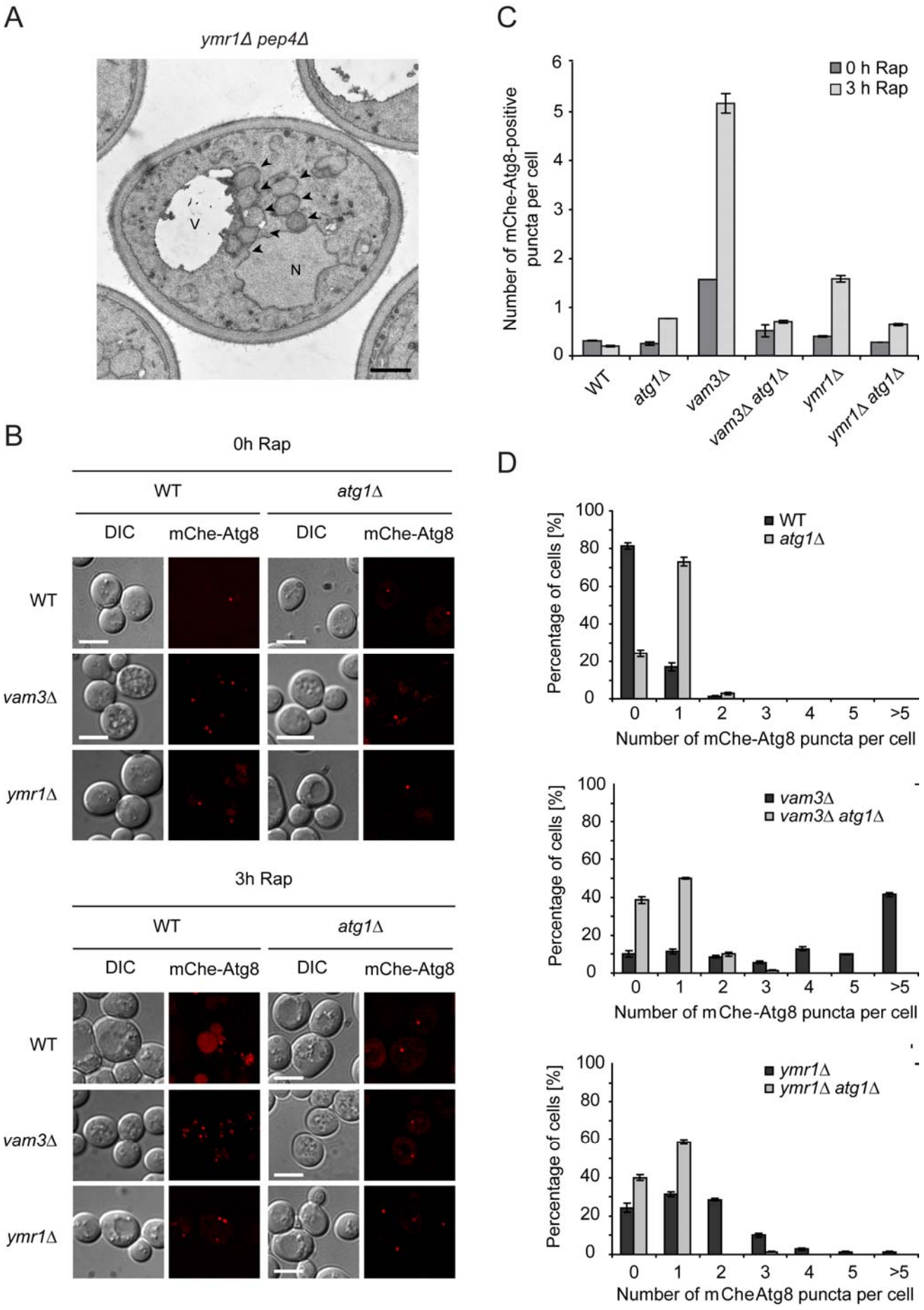
A
ymr1Δ pep4Δ
V
N
B
0h Rap
WT
atg1Δ
DIC
mChe-Atg8
DIC
mChe-Atg8
WT
vam3Δ
ymr1Δ
3h Rap
WT
atg1Δ
DIC
mChe-Atg8
DIC
mChe-Atg8
WT
vam3Δ
ymr1Δ
C
Number of mChe-Atg8-positive puncta per cell
0 h Rap
3 h Rap
0
1
2
3
4
5
6
WT
atg1Δ
vam3Δ
vam3Δ atg1Δ
ymr1Δ
ymr1Δ atg1Δ
D
Percentage of cells [%]
WT
atg1Δ
0
20
40
60
80
100
0
1
2
3
4
5
>5
Number of mChe-Atg8 puncta per cell
Percentage of cells [%]
vam3Δ
vam3Δ atg1Δ
0
20
40
60
80
100
0
1
2
3
4
5
>5
Number of mChe-Atg8 puncta per cell
Percentage of cells [%]
ymr1Δ
ymr1Δ atg1Δ
0
20
40
60
80
100
0
1
2
3
4
5
>5
Number of mCheAtg8 puncta per cell

Figure S3. The *ymr1*Δ cells accumulate autophagosomes. (A) Additional electron microscopy image of a starved *ymr1Δ pep4Δ* (AVY059) cell where several autophagosomes are visible. Sample preparation was performed as detailed in the Experimental procedures. Autophagosomes are indicated with arrowheads. N, nucleus; V, vacuole. Scale bar, 500 nm. (B) WT (SEY6210), *atg1*Δ (WHY1), *vam3*Δ (CWY40), *ymr1*Δ (YMR1Δ), *vam3*Δ *atg1*Δ (ECY023) and *ymr1*Δ *atg1*Δ (ECY115) cells expressing pCumCheAtg8415 were grown to an early log phase and subsequently exposed to rapamycin (Rap) for 3 h. Fluorescence microscopy images of cells in an early log phase and after rapamycin treatment. (B and C) Quantification of mChe-Atg8 foci exhibited by cells before and after autophagy induction with rapamycin, and show in panel B. Effects on the amount of mChe-Atg8 foci per cell caused by the deletion of *ATG1* (C). The average number of mChe-Atg8-positive puncta per cell was determined as described in the Experimental Procedures (B). The graphs represent the average of 3 experiments ± SEM. The diagrams show the percentage of cells with 0, 1, 2, 3, 4, 5 or more than 5 mChe-Atg8 puncta per cell. Note that in the WT, numerous cells do not display a PAS because this structure is highly dynamic and only a defect in one of the *ATG* genes block its progression into a double-membrane vesicle.

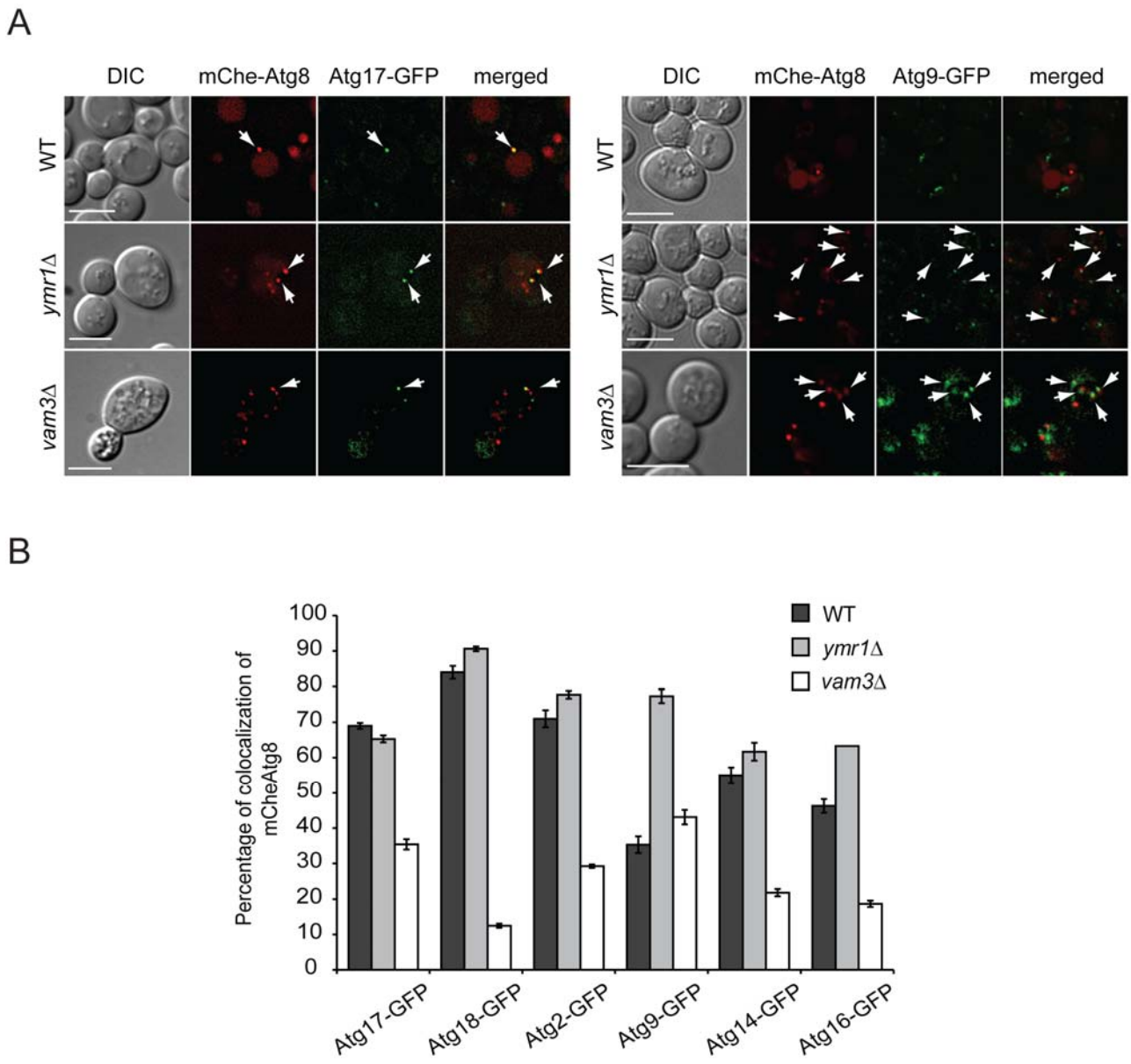

Figure S4. Atg proteins remain associated with the autophagosomes in the *ymr1Δ* strain. WT, *ymr1Δ* and *vam3Δ* strains expressing endogenous Atg17-GFP (PSY167, ECY169 and ECY172) or Atg9-GFP (FRY162, ECY153 and AVY078) and a plasmid expressing mChe-Atg8 under the control of the *CUP1* promoter (pCumCheAtg8415) were grown to an early log phase before being treated with rapamycin for 3 h to trigger autophagy. (A) Fluorescence microscopy images of the various strains after autophagy induction. Arrows highlight colocalizations. (B) Quantification of the co-localization experiment presented in panel A of this figure and Figure 5A by determing the average number of mChe-Atg8 puncta positive for GFP per cell. Error bars represent the SEM. DIC, differential interference contrast. Scale bar, 5 μm.

Table S1. Strains Used in This Study

Name	Genotype	Reference/Origin
AVY059	SEY6210 *ymr1Δ::HIS3 pep4Δ::LEU2*	This study
AVY070	SEY6210 *RFP-APE1::LEU2 SJL3-GFP::HIS3*	This study
AVY078	SEY6210 *ATG9-GFP::KAN vam3Δ::TRP1*	This study
BPY01	SEY6210 *ymr1Δ::HIS3 sjl3Δ::TRP1*	[16]
BPY06	SEY6210 *ymr1Δ::HIS3 sjl2Δ::HIS3*	[16]
CWY40	SEY6210 *vam3Δ::TRP1*	[17]
ECY023	SEY6210 *vam3Δ::TRP1 atg1Δ::URA3*	This study
ECY103	SEY6210 *atg1Δ::HIS3 PEX14-GFP::KAN*	This study
ECY115	SEY6210 *atg1Δ::URA3 ymr1Δ::HIS3*	This study
ECY127	SEY6210 *ymr1Δ::HIS3 OM45-GFP::KAN*	This study
ECY129	SEY6210 *OM45-GFP::TRP1*	This study
ECY131	SEY6210 *PEX14-GFP::TRP1*	This study
ECY133	SEY6210 *atg1Δ::HIS3 OM45-GFP::TRP1*	This study
ECY134	SEY6210 *ymr1Δ::HIS3 PEX14-GFP:: TRP1*	This study
ECY137	SEY6210 *ATG18-GFP::TRP1 ymr1Δ::HIS3*	This study
ECY147	SEY6210 *ATG18-GFP::TRP1 vam3Δ::HIS5*	This study
ECY153	SEY6210 *ATG9-GFP::TRP1 ymr1Δ::HIS3*	This study
ECY155	SEY6210 *ATG2-GFP::TRP1 ymr1Δ::HIS3*	This study
ECY157	SEY6210 *ATG16-GFP::TRP1 ymr1Δ::HIS3*	This study
ECY162	SEY6210 *ATG14-GFP::HIS5 ymr1Δ::URA3*	This study
ECY167	SEY6210 *ATG17-GFP::TRP1*	This study
ECY169	SEY6210 *ATG17-GFP::TRP1 ymr1Δ::HIS3*	This study
ECY172	SEY6210 *ATG17-GFP::TRP1 vam3Δ::URA3*	This study
ECY181	SEY6210 *ymr1Δ::HIS5 RFP-APE1::LEU2 YMR1-GFP::URA3*	This study
ECY182	SEY6210 *ymr1Δ::HIS5 RFP-APE1::LEU2* NΔ*YMR1-GFP::URA3*	This study
ECY183	SEY6210 *ATG2-GFP::HIS5 vam3Δ::TRP1*	This study
ECY184	SEY6210 *ATG14-GFP::HIS5 vam3Δ::TRP1*	This study
ECY185	SEY6210 *ATG16-GFP::HIS5 vam3Δ::TRP1*	This study

ECY189	YTS159 *sjl3Δ::HIS5*	This study
ECY190	YTS159 *ymr1Δ::URA3*	This study
ECY191	SEY6210 *ymr1Δ::HIS5 atg1Δ::URA3 pep4Δ::TRP1*	This study
ECY192	YTS159 *sjl2Δ::URA3 sjl3Δ::HIS5*	This study
ECY193	YTS159 *ymr1Δ::URA3 sjl3Δ::HIS5*	This study
ECY194	YTS159 *sjl2Δ::URA3*	This study
ECY200	YTS159 *ymr1Δ::HIS5 sjl2Δ::URA3*	This study
ECY202	SEY6210 *YMR1-GFP::TRP1 RFP-APE1::LEU2*	This study
ECY207	SEY6210 *ymr1Δ::HIS5 RFP-APE1::LEU2*	This study
ECY208	SEY6210 *YMR1-GFP::TRP1 RFP-APE1::LEU2 atg1Δ::HIS5*	This study
ECY209	SEY6210 *YMR1-GFP::TRP1 RFP-APE1::LEU2 atg4Δ::HIS5*	This study
ECY211	SEY6210 *YMR1-GFP::TRP1 RFP-APE1::LEU2 atg14Δ::HIS5*	This study
ECY212	SEY6210 *YMR1-GFP::TRP1 RFP-APE1::LEU2 vam3Δ::HIS5*	This study
ECY213	SEY6210 *ymr1Δ::HIS5 RFP-APE1::LEU2* $YMR1^{C387S}$*-GFP::URA3*	This study
ECY221	SEY6210 *YMR1-GFP::TRP1 RFP-APE1::LEU2 atg9Δ::URA3*	This study
ECY222	SEY6210 *YMR1-GFP::TRP1 RFP-APE1::LEU2 atg13Δ::URA3*	This study
FRY162	SEY6210 *ATG9-GFP::HIS5 S.p.*	[18]
FRY300	YTS159 *atg9Δ0*	[8]
JGY130	SEY6210 s*jl2Δ::HIS3*	[16]
JGY131	SEY6210 *sjl3Δ::TRP1*	[16]
JGY132	SEY6210 s*jl2Δ::HIS3 sjl3Δ::TRP1*	[16]
KTY148	SEY6210 *ATG16-GFP::HIS5*	[7]
MZY089	SEY6210 *atg8Δ::HIS5 pATG8-GFP-Atg8::LEU2*	This study
MZY090	SEY6210 *atg8Δ::HIS5 ymr1Δ::TRP1 pATG8-GFP-Atg8::LEU2*	This study
PSY62	SEY6210 *ATG18-GFP::HIS5*	[7]
PSY102	SEY6210 *ATG2-GFP::HIS5*	This study

PSY142	SEY6210 *ATG14-GFP::HIS5*	[18]
SEY6210	*MATa ura3-52 leu2-3,112 his3-Δ200 trp1-Δ901 lys2-801 suc2-Δ9 mel GAL*	[19]
TVY1	SEY6210 *pep4Δ::LEU2*	[20]
WHY1	SEY6210 *atg1Δ::HIS3*	[21]
YMR1Δ	SEY6210 *ymr1Δ::HIS3*	[16]
YTS113	SEY6210 *atg1Δ::HIS5 pep4Δ::LEU2*	[21]
YTS159	*MATα his3Δ1 leu2Δ0 lys2Δ0 ura3Δ0 pho13Δ::KAN pho8::PHO8Δ60*	[22]

Supplemental References

1. Gueldener, U., Heinisch, J., Koehler, G.J., Voss, D., and Hegemann, J.H. (2002). A second set of *loxP* marker cassettes for Cre-mediated multiple gene knockouts in budding yeast. Nucleic Acids Res *30*, e23.

2. Abeliovich, H., Zhang, C., Dunn, W.A., Jr., Shokat, K.M., and Klionsky, D.J. (2003). Chemical genetic analysis of Apg1 reveals a non-kinase role in the induction of autophagy. Mol Biol Cell. *14*, 477-490.

3. Longtine, M.S., McKenzie, A., III, Demarini, D.J., Shah, N.G., Wach, A., Brachat, A., Philippsen, P., and Pringle, J.R. (1998). Additional modules for versatile and economical PCR-based gene deletion and modification in *Saccharomyces cerevisiae*. Yeast *14*, 953-961.

4. Sikorski, R.S., and Hieter, P. (1989). A system of shuttle vectors and yeast host strains designed for efficient manipulation of DNA in *Saccharomyces cerevisiae*. Genetics *122*, 19-27.

5. Kadowaki, H., Kadowaki, T., Wondisford, F.E., and Taylor, S.I. (1989). Use of polymerase chain reaction catalyzed by Taq DNA polymerase for site-specific mutagenesis. Gene *76*, 161-166.

6. Kim, J., Huang, W.-P., Stromhaug, P.E., and Klionsky, D.J. (2002). Convergence of multiple autophagy and cytoplasm to vacuole targeting components to a perivacuolar membrane compartment prior to de novo vesicle formation. J Biol Chem *277*, 763-773.

7. Stromhaug, P.E., Reggiori, F., Guan, J., Wang, C.-W., and Klionsky, D.J. (2004). Atg21 is a phosphoinositide binding protein required for efficient lipidation and localization of Atg8 during uptake of aminopeptidase I by selective autophagy. Mol Biol Cell *15*, 3553-3566.

8. Mari, M., Griffith, J., Rieter, E., Krishnappa, L., Klionsky, D.J., and Reggiori, F. (2010). An Atg9-containing compartment that functions in the early steps of autophagosome biogenesis. J Cell Biol *190*, 1005-1022.

9. Geng, J., Baba, M., Nair, U., and Klionsky, D.J. (2008). Quantitative analysis of autophagy-related protein stoichiometry by fluorescence microscopy. J Cell Biol *182*, 129-140.

10. van der Vaart, A., Griffith, J., and Reggiori, F. (2010). Exit from the Golgi is required for the expansion of the autophagosomal phagophore in yeast *Saccharomyces cerevisiae*. Mol Biol Cell *21*, 2270-2284.

11. Harding, T.M., Morano, K.A., Scott, S.V., and Klionsky, D.J. (1995). Isolation and characterization of yeast mutants in the cytoplasm to vacuole protein targeting pathway. J Cell Biol *131*, 591-602.

12. Wiesli, P., Bernays, R., Brandle, M., Zwimpfer, C., Seiler, H., Zapf, J., G, A.S., and Schmid, C. (2005). Effect of pituitary surgery in patients with acromegaly on adiponectin serum concentrations and alanine aminotransferase activity. Clin Chim Acta *352*, 175-181.

13. Hutchins, M.U., Veenhuis, M., and Klionsky, D.J. (1999). Peroxisome degradation in *Saccharomyces cerevisiae* is dependent on machinery of macroautophagy and the Cvt pathway. J Cell Sci *112*, 4079-4087.

14. Cheong, H., and Klionsky, D.J. (2008). Biochemical methods to monitor autophagy-related processes in yeast. Meth Enzymol *451*, 1-26.

15. Kanki, T., Kang, D., and Klionsky, D.J. (2009). Monitoring mitophagy in yeast: the Om45-GFP processing assay. Autophagy *5*, 1186-1189.

16. Parrish, W.R., Stefan, C.J., and Emr, S.D. (2004). Essential role for the myotubularin-related phosphatase Ymr1p and the synaptojanin-like phosphatases Sjl2p and Sjl3p in regulation of phosphatidylinositol 3-phosphate in yeast. Mol Biol Cell *15*, 3567-3579.

17. Wang, C.-W., Stromhaug, P.E., Shima, J., and Klionsky, D.J. (2002). The Ccz1-Mon1 protein complex is required for the late step of multiple vacuole delivery pathways. J Biol Chem *277*, 47917-47927.

18. Reggiori, F., Tucker, K.A., Stromhaug, P.E., and Klionsky, D.J. (2004). The Atg1-Atg13 complex regulates Atg9 and Atg23 retrieval transport from the pre-autophagosomal structure. Dev Cell *6*, 79-90.

19. Robinson, J.S., Klionsky, D.J., Banta, L.M., and Emr, S.D. (1988). Protein sorting in *Saccharomyces cerevisiae*: isolation of mutants defective in the delivery and processing of multiple vacuolar hydrolases. Mol Cell Biol *8*, 4936-4948.

20. Gerhardt, B., Kordas, T.J., Thompson, C.M., Patel, P., and Vida, T. (1998). The vesicle transport protein Vps33p is an ATP-binding protein that localizes to the cytosol in an energy-dependent manner. J Biol Chem. *273(25)*, 15818-15829.

21. Shintani, T., Huang, W.-P., Stromhaug, P.E., and Klionsky, D.J. (2002). Mechanism of cargo selection in the cytoplasm to vacuole targeting pathway. Dev Cell *3*, 825-837.

22. Cheong, H., Nair, U., Geng, J., and Klionsky, D.J. (2008). The Atg1 kinase complex is involved in the regulation of protein recruitment to initiate sequestering vesicle formation for nonspecific autophagy in *Saccharomyces cerevisiae*. Mol Biol Cell *19*, 668-681.